Supporting information for

Detailed Structure Analysis of Atomic Positions and Defects in Zirconium Metal-Organic Frameworks

Sigurd Øien[†], David Wragg[†], Helge Reinsch[†], Stian Svelle[†], Silvia Bordiga[†,‡], Carlo Lamberti[‡,§] and Karl Petter Lillerud*[,†]

[†]*Department of Chemistry, University of Oslo, P.O. box 1037, N-0371 Oslo, Norway* and
[‡]*Department of Chemistry, NIS and INSTM Reference Centre, Via Quarello 15, I-10135 Torino, Italy*
[§]*Southern Federal University, Zorge Street 5, 344090 Rostov-on-Don, Russia*

Synthesis

All chemicals were purchased from Sigma-Aldrich and used without further purification with the exception of DMF (≥99.5 %, Merck) which was purified using a MBraun MB-SPS-800 encapsulated solvent purification system.

Synthesis of UiO-66: $ZrCl_4$ (303 mg, 1.30 mmol), $HCl_{(aq)}$ (35 %, 92 µl, 1.03 mmol HCl, 3.87 mmol H_2O), benzoic acid (4.70 mg, 38.5 mmol) and terephthalic acid (224 mg, 1.33 mmol) were dissolved in hot dimethylformamide (10 mL, 0.13 mol). The clear solution was transferred to a 25 mL Erlenmeyer flask which had been submerged in 2.0 M KOH(aq) overnight, and set to static heating at 110 °C for 48 hours. A loose lid was placed on the flask to allow for evaporation of volatile byproducts. Single crystals of approximately (10 µm)^3 were then carefully recovered from the inclining walls of the flask. The majority of the product formed a membrane of intergrown crystals on the bottom of the flask. The crystals were washed twice in 10 mL portions of DMF, and three times in 10 mL portions of THF.

Synthesis of UiO-67: $ZrCl_4$ (240 mg, 1.03 mmol), $HCl_{(aq)}$ (35 %, 83 µl, 0.83 mmol HCl, 3.10 mmol H_2O), benzoic acid (3.80 mg, 31.0 mmol) and biphenyl-4,4'-dicarboxylic acid (253 mg, 1.03 mmol) were dissolved in hot dimethylformamide (20 mL, 0.26 mol). The clear solution was transferred to a 25 mL Erlenmeyer flask which had been submerged in 2.0 M KOH(aq) overnight, and set to static heating at 120 °C for 48 hours. A loose lid was placed on the flask to allow for evaporation of volatile byproducts. Single crystals of approximately (70 µm)^3 were then carefully recovered from the inclining walls of the flask. The majority of the product formed a membrane of intergrown crystals on the bottom of the flask. The crystals were washed twice in 10 mL portions of DMF, and three times in 10 mL portions of THF.

Crystallographic refinement

The data was integrated and scaled using SAINT and SADABS[1]. The structures were solved with ShelxS and refined with ShelxL[2]. All structure refinements are made independently and without restraints. In UiO-66, the aromatic hydrogen was modelled on its neighboring C, but in UiO-67 it was refined directly from the Fourier transform electron density map. Occupancy of the linker molecules and the µ3-O and OH were allowed to refine freely. Disordered solvent molecules in the pores were modelled with partially occupied oxygen atoms. These atoms tend to be un-physical with very large anisotropic displacement factors and occupancy factors above 1.0. This has led to some A and B-level alerts in checkcif, but we think it's justified to make a realistic structure refinement. We have also made supplementary structure refinements using Platon/SQUEEZE to correct for disordered solvent in the pores in the more conventional way, indicated with an S in the table of results (table 1).

We found no indications of the high symmetry being broken, indicating that there's no order in the pores except for slightly higher solvent occupancy in the adsorption site, and no long-range order µ3-O/OH arrangement.

The UiO-67 linker is modelled out of the conjugation plane, due to the rocking motion of the aromatic rings. This gives a more accurate modeling of the electron density than ellipsoids centered in the plane. From the electron density map we know the occupancy is largest in the plane, so in the thermodynamically favored configuration the phenyl is coplanar with the carboxylate group.

The H atom in the µ3-OH unit is not possible to include in the model. It is a proton with half site occupancy, and the site is also a strong adsorption site.

Table 1. Summary of single crystal measurements and refinement. A and B indicates separate measurements. S indicates refinement using Platon/SQUEEZE to eliminate disordered solvent molecules from the pores. The complete refinement details, along with standard deviations can be found in the cif files.

Data set	UiO-66 A	UiO-66 A S	UiO-66 B	UiO-66 B S	UiO-67 A	UiO-67 A S	UiO-67 B	UiO-67 B S
a	20.7465	20.7465	20.7411	20.7411	26.8809	26.8809	26.8858	26.8858
Zr – μ^3O	2.064	2.065	2.066	2.062	2.059	2.058	2.059	2.057
Zr – μ^3OH	2.256	2.259	2.269	2.258	2.254	2.252	2.251	2.246
O-OH	0.607	0.607	0.621	0.618	0.628	0.628	0.624	0.625
Zr - O_{carb}	2.213	2.21	2.216	2.214	2.218	2.218	2.219	2.219
Zr - O_{def}	2.225	2.228	2.221	2.216				
C-O_{carb}	1.258	1.259	1.265	1.261	1.269	1.268	1.268	1.268
μ_3-OH occupancy	0.54	0.51	0.50	0.54	0.52	0.52	0.51	0.53
Linkers occupancy	72.7	71.4	73.5	71.4	100	100	100	100
Reflections	739	739	728	728	1514	1514	1520	1520
Parameters	53	38	50	38	55	55	59	55
Restraints	0	0	0	0	0	0	0	0
F000	3779	2848	3570	2848	4192	4192	4254	4192
(sin θ)/λ	0.713	0.713	0.713	0.713	0.712	0.712	0.714	0.714
R_{int}	3.7	3.7	3.9	3.9	2.7	2.7	3.6	3.6
R_1 ($I>2\sigma_{(I)}$)	2.3	2.0	2.9	2.4	2.1	1.8	2.0	1.7
wR	7.1	6.0	9.1	6.5	5.5	5.0	5.5	4.8
S	1.11	1.16	1.15	1.07	1.05	1.17	1.11	1.13

Diffuse scattering peaks of UiO-66

A few diffuse scattering peaks were observed in the diffraction frames of UiO-66. Examples are shown in figures 1-3.

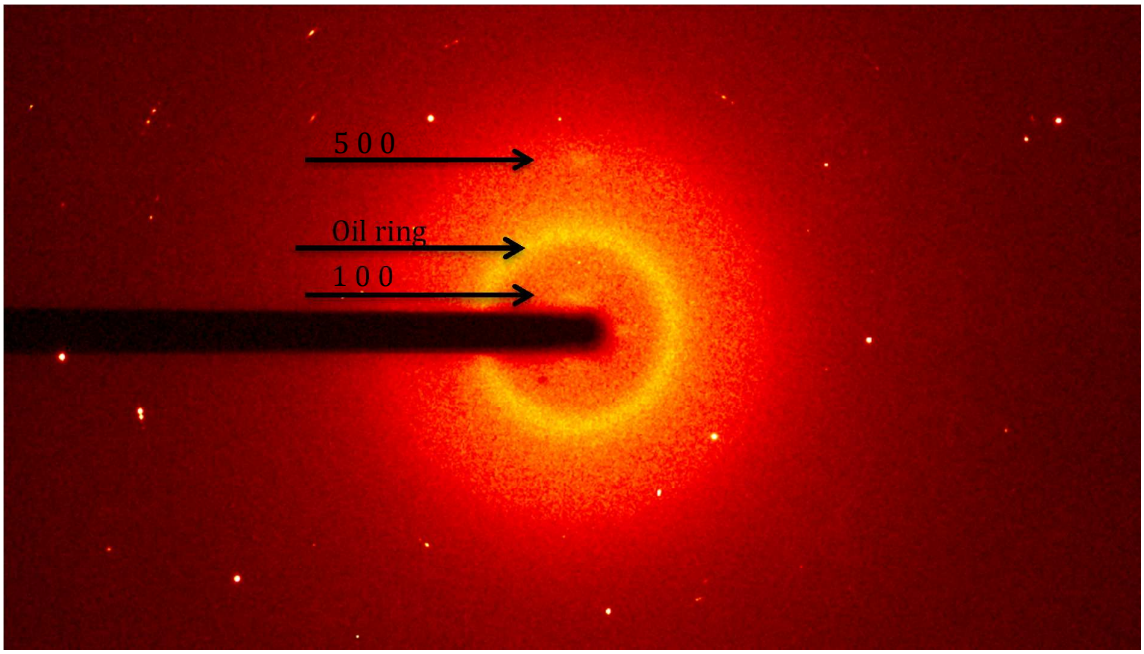

Figure 1. Partial diffraction frame (width = 0.5° θ), showing broad, diffuse reflections 1 0 0 and 5 0 0.

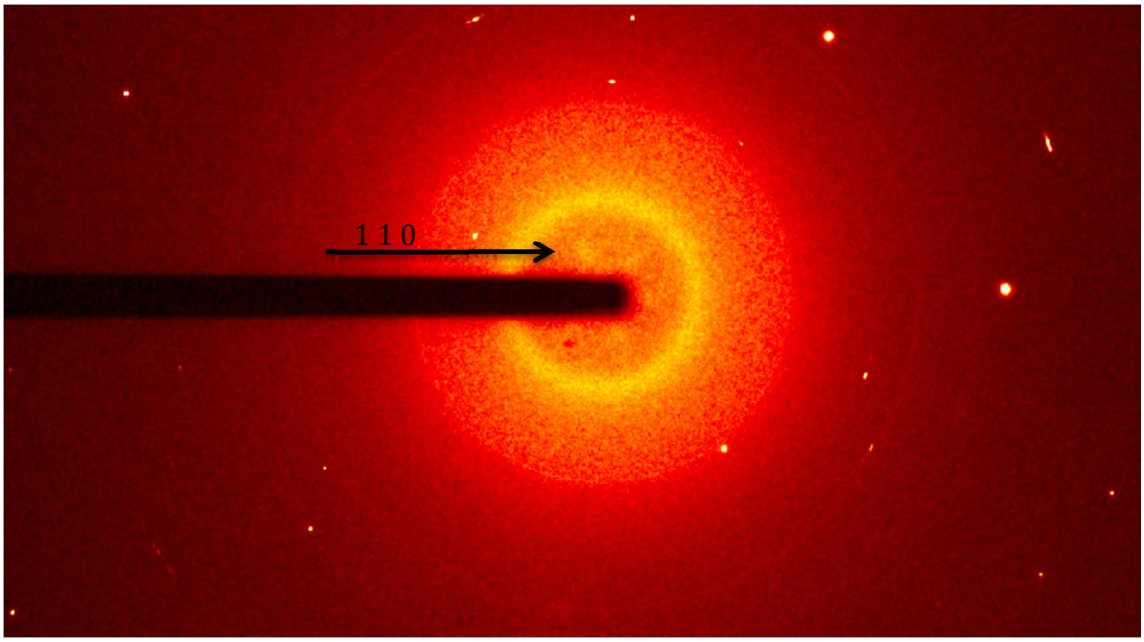

Figure 2. Partial diffraction frame (width = 0.5° θ), showing broad, diffuse reflections 1 1 0.

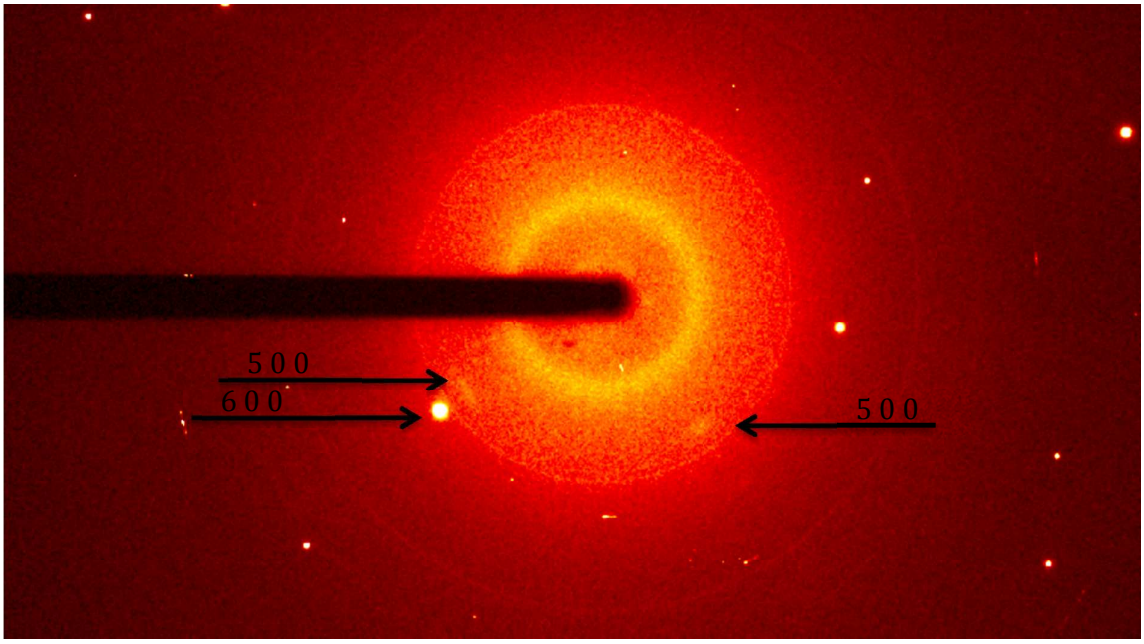

Figure 3. Partial diffraction frame (width = 0.5° θ), showing broad, diffuse reflections 5 0 0.

Thermogravimetric analysis

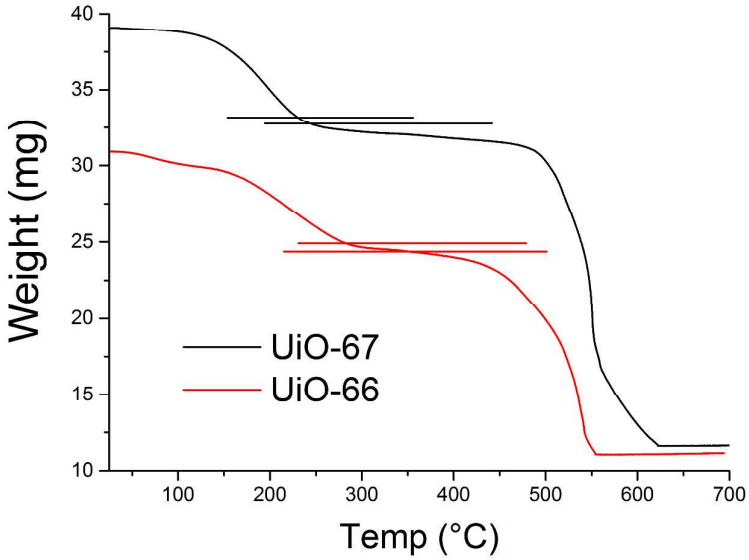

Figure 4. TGA curves of UiO-66 and UiO-67, acquired under a 20 mL/min flow of dry air. Expected masses of a defect-free material is indicated with horizontal lines.

Powder x-ray diffraction patterns and thermogravimetric measurements were made on the bulk samples from which the single crystals were harvested. TGA curves were recorded on a Stanton Redcroft TGA, in a 20 mL/min flow of dry synthetic air with a heating rate of 5 °C per minute.

TGA curves show a deviation from expected mass ratios (figure 4). Assuming the residual mass above 600 °C is ZrO_2 (found in PXRD), the horizontal lines represent the mass of a MOF with 100% linker occupancy. This deviance can be explained by the fact that there could be significant differences between the single crystals and the bulk sample. The intergrown membrane of crystallites in the bulk sample has had different growth conditions than the single crystals on the flask wall, and there may be other solids present in the sample, such as amorphous Zr terephthalate which cannot readily be separated from the MOF. For UiO-66 there is a higher mass than expected evaporating/burning between 400 and 550. For UiO-67 it is lower than expected. The TGA curves, considering the consistency of the X-ray data, strongly indicates a presence of amorphous phases, probably by-products of synthesis that could not be separated from the MOF through regular work-up procedures.

PXRD refinement

The structural information obtained by single-crystal X-ray diffraction was used as a starting point for Rietveld-refinements. Data was acquired on a Bruker D8 Discover with Cu $K_{\alpha 1}$-radiation in reflection geometry. The employed software was TOPAS 4.2.[3]. While structural disorder regarding linker molecules and oxygen atoms was observed in the SC-data, the Rietveld-refinements showed no such phenomena. The reason for this is most probably the averaging over a large number of crystals and the higher temperature of the PXRD-measurement compared to SC-diffraction. Due to this only the averaged positions are determined. Residual electron density was located inside the framework's cavities by Fourier-synthesis and was attributed to partially occupied oxygen atoms. However, these extra-framework atoms represent placeholders for any kind of molecules that might reside inside the pores. The atomic positions were freely refined as well as the linker molecule's occupancies. After the refinement had converged, the final values indicated reasonable agreement with SC-data. The final Plots are shown in Figure 5 and 6, some relevant values are summarised in Table 2. Asymmetric units and important bond lengths are displayed in Figure 7 and Tables 3 and 4.

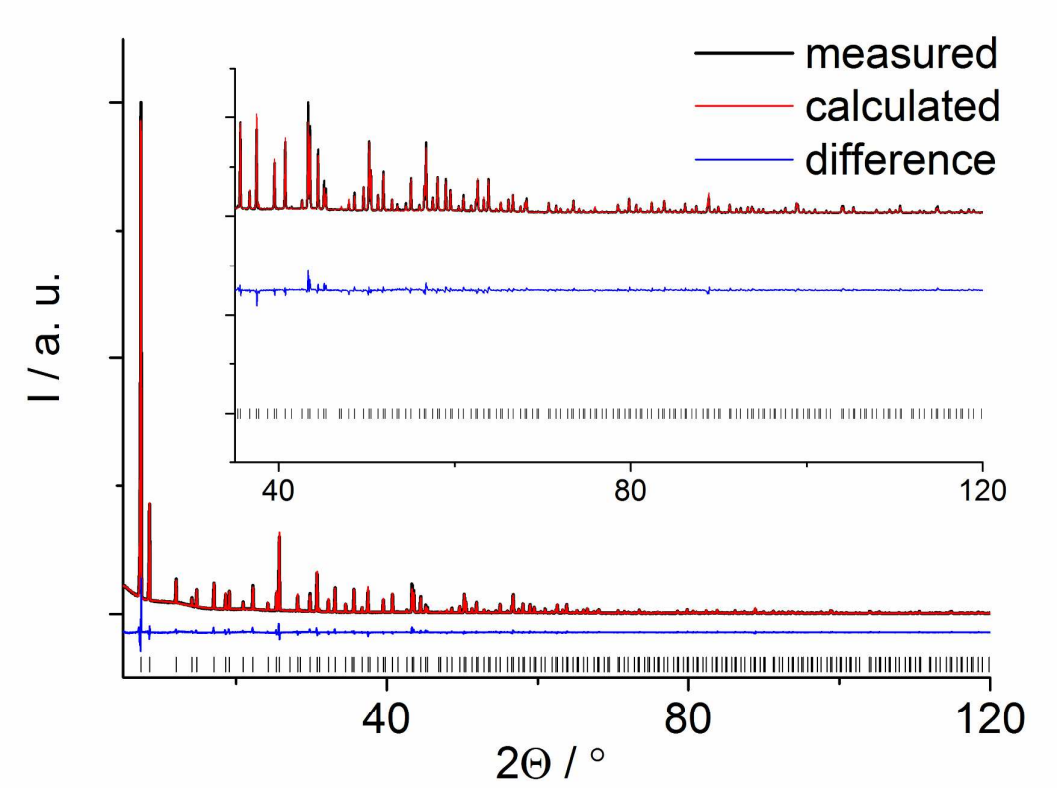

Figure 5. Final plot of the Rietveld-refinement for UiO-66. Measured data is shown in black, theoretical fit is shown in red and the blue line gives the difference curve. Vertical bars mark the Bragg-reflection positions.

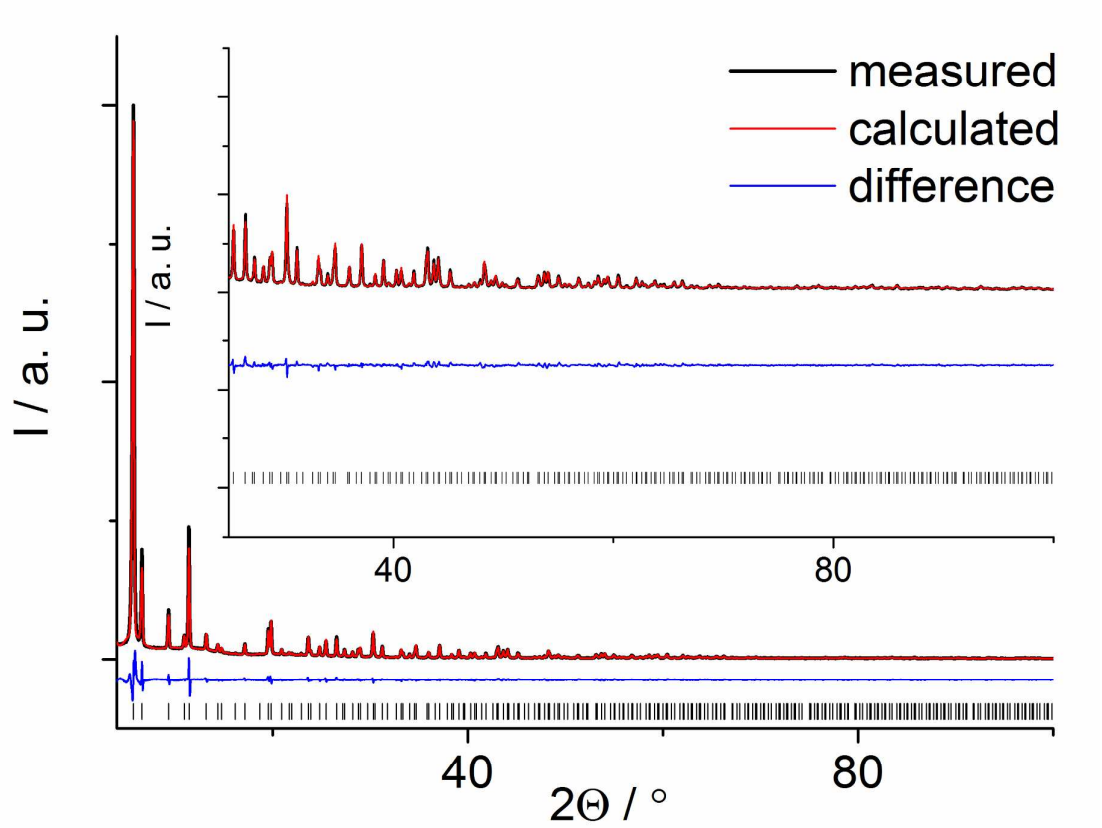

Figure 6. Final plot of the Rietveld-refinement for UiO-67. Measured data is shown in black, theoretical fit is shown in red and the blue line gives the difference curve. Vertical bars mark the Bragg-reflection positions.

Table 2: Important Values and Figures of Merit obtained by Rietveld-refinement.

Compound	UiO-66	UiO-67
Space Group	*Fm-3m*	*Fm-3m*
$a = b = c$	20.7587(1)	26.8552(9)
Cell Volume [Å^3]	8945.5(1)	19368.1(11)
R_{WP} [%]	8.8	9.2
R_{Bragg} [%]	3.5	2.0
GoF	1.6	1.9
Linker Occupancy [%]	75.9(7)	100(1)

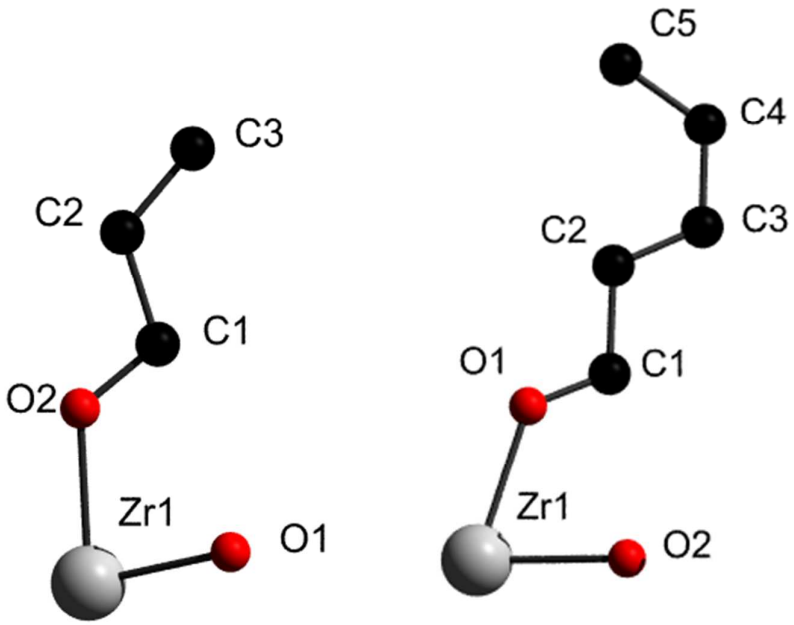

Figure 7. Asymmetric units of UiO-66 (left) and UiO-67 (right) with numbering scheme used in table 3 and 4. Oxygen atoms representing guest molecules are omitted for clarity.

Table 3: Relevant bond lengths observed for UiO-66.

Zr1	O1	2.128(6)
	O2	2.235(4)
O2	C1	1.279(7)
C1	C2	1.508(9)
C2	C3	1.389(9)
C3	C3	1.410(8)

Table 4: Relevant bond lengths observed for UiO-67.

Zr1	O2	2.126(9)
	O1	2.261(5)
O1	C1	1.243(16)
C1	C2	1.493(17)
C2	C3	1.376(15)
C3	C4	1.417(15)
C4	C5	1.399(12)
C5	C5	1.517(11)

References

(1) AXS, B. Madison, Wisconsin, USA,, 2014.
(2) Sheldrick, G. M. *Acta Crystallogr A* **2008**, *64*, 112.
(3) Coelho, A. A.; Evans, J.; Evans, I.; Kern, A.; Parsons, S. *Powder Diffr.* **2011**, *26*, S22.